*Molecular Vision* 2009; 15:1374-1382 <http://www.molvis.org/molvis/v15/a145>
Received 10 February 2009 | Accepted 21 June 2009 | Published 17 July 2009



# Adeno-associated virus serotype-9 efficiently transduces the retinal outer plexiform layer

**Bo Lei,[1,2] Keqing Zhang,[2] Yongping Yue,[3] Arkasubhra Ghosh,[3] Dongsheng Duan[3]**

*[1]Department of Ophthalmology, the First Affiliated Hospital of Chongqing Medical University, Chongqing Key Laboratory of Ophthalmology, Chongqing, China; [2]Department of Veterinary Medicine and Surgery, Department of Ophthalmology, Mason Eye Institute, University of Missouri, Columbia, MO; [3]Department of Molecular Microbiology and Immunology, University of Missouri, Columbia, MO*

**Purpose:** Adeno-associated virus serotype-9 (AAV-9) is a promising gene delivery vector. In this study, we evaluated AAV-9 transduction in the mouse retina.

**Methods:** Three different AAV vectors were used in our study: AAV-9.RSV.AP, AAV-9.CMV.eGFP, and AAV-9.CMV.ΔR4–23/ΔC. In these vectors, two different promoters (the cytomegalovirus promoter-CMV promoter and the Rous sarcoma virus-RSV promoter) were used to express three different transgenes including the alkaline phosphatase (*AP*) gene, the enhanced green fluorescent protein (*eGFP*) gene, and a therapeutic microdystrophin gene (the Δ*R4–23/ΔC*). Specifically, 1 µl AAV-9 reporter gene vectors ($1\times10^9$ viral genome particles of AAV-9.RSV.AP or $1\times10^{10}$ viral genome particles of AAV-9.CMV.eGFP) were administered subretinally to young (2–3-week-old), adult (3-month-old), and old (12-month-old) *C57BL/6J* mice. To evaluate AAV-9 transduction in a diseased retina, we injected subretinally $1\times10^9$ viral genome particles of AAV-9.CMV.ΔR4–23/ΔC to *mdx$^{3cv}$* mice, which we used as a model for Duchenne muscular dystrophy (DMD). Transgene expression was examined by histochemical as well as immunofluorescence staining at three and five weeks after injection. Electroretinograms were recorded five weeks after subretinal AAV-9.RSV.AP injection.

**Results:** Subretinal injection yielded widespread transduction throughout the retina in all age groups. Robust expression was seen in the retinal pigment epithelium, outer nuclear layer, and in Müller cells. Interestingly a synaptic layer, the outer plexiform layer (OPL), also showed intensive expression. Transduction of the synaptic layer was further confirmed by immunostaining for C-terminal binding protein 2 (CtBP2), a marker for the photoreceptor synaptic ribbon. Dystrophin is normally expressed in the OPL photoreceptor terminals. This expression is lost in DMD patients and *mdx$^{3cv}$* mice. Consistent with our findings in normal mice, we observed efficient microdystrophin expression in the OPL after AAV-9.CMV.ΔR4–23/ΔC infection. At five weeks after subretinal delivery of AAV-9.RSV.AP, no morphology or ERG abnormalities were observed.

**Conclusions:** We demonstrated that AAV-9 is a potent vector for retinal gene delivery. Furthermore, subretinal AAV-9 administration did not cause appreciable acute retinal damages. In summary, AAV-9-mediated OPL transduction holds promise for treating diseases that primarily affect this layer.

Adeno-associated virus (AAV) is a single-stranded DNA virus. AAV-mediated gene therapy has successfully corrected several degenerative retinal diseases in animal models [1-4]. Recent successes in Leber congenital amaurosis phase I trials have provided the first clinical proof that AAV vector holds great promise in treating retinal diseases [5-8].

Recombinant AAV vectors are generated by replacing the endogenous viral genome with a therapeutic or marker gene expression cassette. The prototype AAV vector is based on AAV serotype-2 (AAV-2). In the last few years, several new AAV serotypes have been developed [9]. Due to the differences in the cellular transduction pathway, these new serotypes have opened additional avenues for tailoring AAV gene therapy to specific clinical applications. Previous studies have evaluated AAV serotypes 1–9 in the retina [3,10-13]. It was found that subretinal injection transduces the outermost retinal structures, such as retinal pigment epithelium (RPE) and the photoreceptors, while intravitreal injection transduces ganglion cells in the innermost layer. Pathology in the retinal synaptic layers such as the outer plexiform layer (OPL) is associated with a wide range of retinal diseases [14-18]. Two recent studies suggest that AAV may transduce the OPL [12, 19]. However, these studies did not explicitly explore the specificity of OPL transduction. Considering the importance of the OPL in retinal diseases, a thorough and more focused study would be necessary to establish AAV transduction in the OPL. Such efforts would likely open the door for AAV-mediated OPL disease gene therapy.

AAV serotype-9 (AAV-9) was discovered a few years ago from human tissue [9,20]. Due to its unique serological property, it was classified as clade F, a clade distinctive from

Correspondence to: Bo Lei, Department of Ophthalmology, The First Affiliated Hospital of Chongqing Medical University, 1 You Yi Road, Yu Zhong District, Chongqing, 400016, China; Phone: 0086 23 68485440; FAX: 0086 23 68485440; email: bolei99@126.com

all known AAVs [20]. AAV-9 has been shown to efficiently transduce several tissues including the heart, liver, lung, kidney, pancreas, and skeletal muscle [21-27]. Furthermore, it was reported recently that AAV-9 is capable of bypassing the blood-brain barrier and efficiently targeting cells of the central nervous system [21]. This unique feature may enable the development of gene therapies for a range of neurodegenerative diseases. Two studies evaluated AAV-9 transduction in the retina following subretinal administration [12,13]. Both studies demonstrated efficient transduction of RPE and Müller cells [12,13]. Interestingly, one group showed photoreceptor transduction [12]. However, the other group did not detect photoreceptor transduction [13]. The reasons for these differences are not clear but may relate to animal age, the promoter and the reporter gene used, and the time frame of observation. To further characterize AAV-9 transduction in the retina, we performed a comprehensive study in young (2–3-week-old), adult (3-month-old), and old (12-month-old) mice using either an Rous sarcoma virus promoter (RSV) driving alkaline phosphatase reporter gene vector (AAV-9.RSV.alkaline phosphate [AP]) or a Cytomegalovirus promoter (CMV) driving enhanced green fluorescent protein (AAV-9.CMV.enhanced green fluorescent protein [eGFP]) reporter gene vector. To further extend the study, we also evaluated subretinal delivery of a therapeutic microdystrophin vector (AAV-9.CMV.ΔR4–23/ΔC) in adult *mdx*$^{3cv}$ mice, a model for Duchenne muscular dystrophy (DMD). We observed widespread transduction throughout the retina following subretinal injection. Interestingly, we observed remarkable transduction in the synaptic OPL irrespective of the vector used. Colocalization experiments with a marker of the photoreceptor presynaptic ribbon further confirmed the OPL transduction. To our knowledge, this is the first demonstration of efficient retinal synaptic layer transduction by an AAV vector. Besides tissue tropism, we also evaluated acute toxicity of subretinal AAV-9 injection. Our results suggest that subretinal AAV-9 delivery was not associated with deleterious effect on retinal morphology and electroretinogram (ERG) function.

## METHODS

*Experimental animals:* All experiments were conducted in accordance with the Association for Research in Vision and Ophthalmology Statement for the Use of Animals in Ophthalmic and Vision Research. The experimental protocols were reviewed and approved by institutional animal care and use committee at the University of Missouri. *C57BL/6J* and *mdx*$^{3cv}$ mice were originally purchased from The Jackson Laboratory (Bar Harbor, ME). Experimental mice were obtained from local breeding colonies. All mice were housed in specific pathogen-free (SPF) animal care facilities and kept under a 12 h:12 h light-dark cycle (25 lx) with free access to food and water.

*Recombinant AAV-9 production:* AAV-9 stocks were generated using an adenoviral free triplasmid transfection protocol described previously [22,23]. Briefly, 70% to 80% confluent 293 cells were cotransfected with a *cis*-plasmid, a pRep2/Cap9 helper plasmid (a gift from Dr. James M. Wilson, University of Pennsylvania, Philadelphia, PA) and an adenoviral helper plasmid (pHelper; Stratagene, La Jolla, CA). Crude viral lysate was harvested 72 h later and purified through two rounds of CsCl isopycnic ultracentrifugation. Purified virus was dialyzed through three exchanges of HEPES buffered saline at 4 °C. Viral titer determination and quality control were performed as described before [22,23]. Briefly, viral DNA was extracted and slot blot hybridization was performed using P32-labeled radioactive probe. Vector genome was determined according to the plasmid copy number standards. The absence of significant wild type AAV contamination was confirmed by immunofluorescence staining with an antibody that recognizes AAV Rep protein.

The *cis*-plasmids (pcisRSV.AP, pcisCMV.eGFP, and pcisCMV.ΔR4–23/ΔC) have been reported previously [24, 25]. pcisRSV.AP expresses the heat-resistant human placental AP gene under the transcriptional control of the RSV promoter and the SV40 polyadenylation signal (pA). pcisCMV.eGFP expresses the eGFP gene under the transcriptional control of the CMV promoter and the SV40 pA. pcisCMV.ΔR4–23/ΔC encodes a highly abbreviated ΔR4–23/ΔC human microdystrophin gene under the transcriptional control of the CMV and the SV40 pA [28]. Specifically, a large portion of the dystrophin rod domain (from spectrin-like repeat 4 to 23) and the entire C-terminal domain are deleted. The recombinant AAV vectors are called AAV-9.RSV.AP, AAV-9.CMV.eGFP, and AAV-9.CMV.ΔR4–23/ΔC.

*Subretinal injection:* AAV-9.RSV.AP and AAV-9.CMV.eGFP injection were delivered to young (2- to 3-week-old), adult (3-month-old), and old (12-month-old) *C57BL/6J* mice. AAV-9.CMV.ΔR4–23/ΔC injection was delivered to 3-month-old adult *mdx*$^{3cv}$ mice. HEPES-buffered saline was used as vehicle control in a subset of animals.

Mice were given 1% atropine eyedrops 3 h before they were anesthetized with an intraperitoneal injection of a mixture of 75 mg/kg ketamine and 13.6 mg/kg xylazine. Following general anesthesia, 2.5% phenylephrine hydrochloride eyedrops were applied. One drop of 1% proparacaine hydrochloride was administered as local anesthesia, followed by 2.5% hydroxypropyl methylcellulose. Subretinal injection was performed according to a previous publication with modifications [29]. Briefly, an aperture within the pupil area was made through the superior cornea with a 30-gauge needle. A 33-gauge blunt needle mounted on a 10-µl syringe was introduced through the corneal opening, avoiding the lens and penetrating the neuroretina to reach the posterior subretinal space. The NanoFil™ sub-microliter injection system (WPI, Sarasota, FL) was used to inject 1 µl

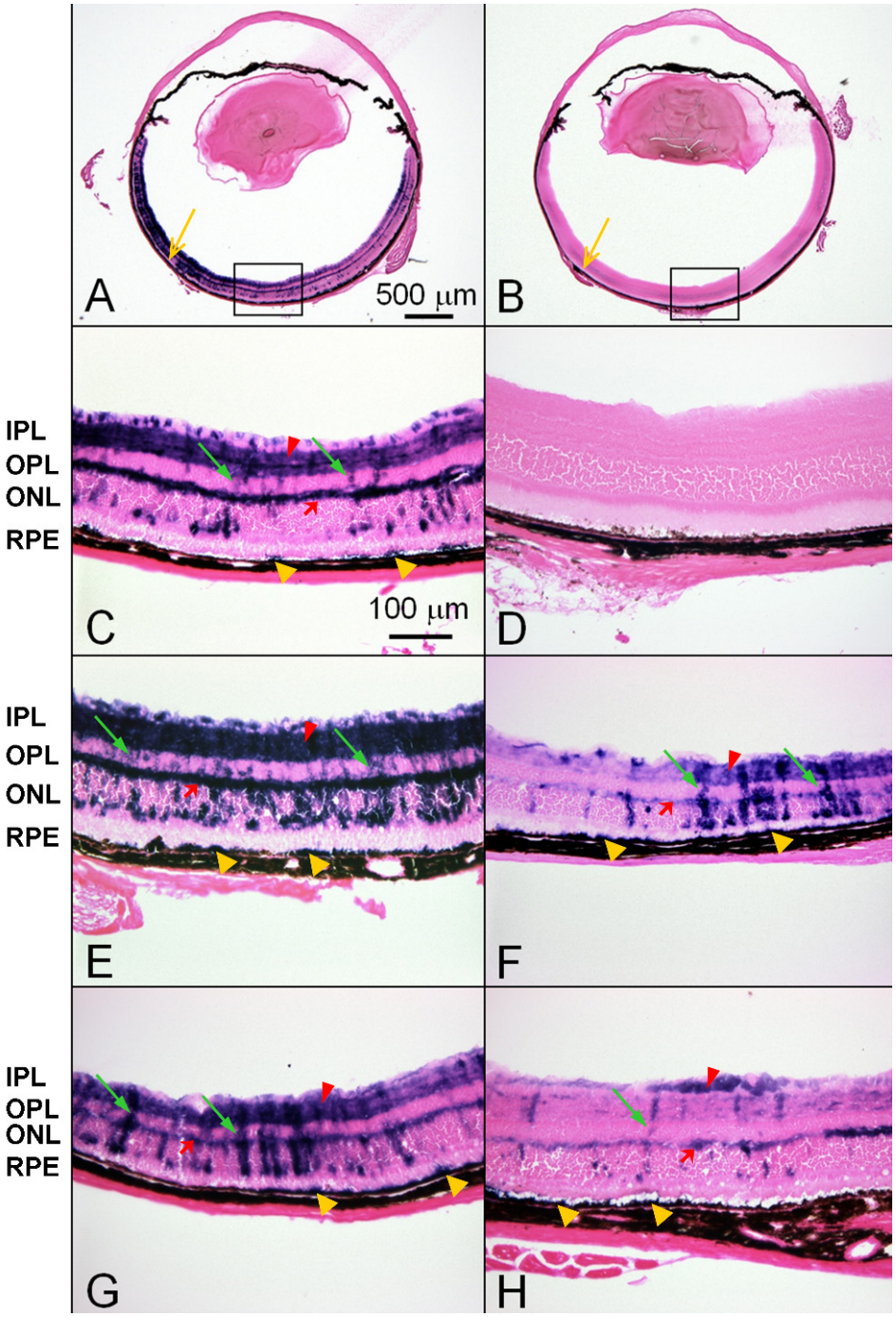


Figure 1. Representative retinal cross sections of *C57BL/6J* mice after subretinal delivery of AAV-9.RSV.AP. Panels **A** and **B** show global view of AAV-9 transduction in adult (3-month-old) *C57BL/6J* mouse eyes at 5 weeks after subretinal AAV-9.RSV.AP injection (**A**) and HEPES buffer injection (**B**). Yellow arrows indicate the injection sites. Panels **C** and **D** show the enlarged retinal sections of the boxed regions in **A** and **B**, respectively. Panels **E** and **F** are representative retinal sections obtained from young (3-week-old) mice at 3 weeks after subretinal injection. **E** shows the area close to the injection site while **F** shows an area distant from the injection site. Panels **G** and **H** are representative retinal sections obtained 5 weeks after subretinal injection in a 12-month-old mouse. **G** shows the area close to the injection site while **H** shows an area distant from the injection site. Similar AP expression pattern can be seen in all AAV-9.RSV.AP-injected eyes. Dark blue AP staining is readily visible throughout the entire retina. The RPE, ONL, INL, and RGC layers show punctate staining. AP-positive Müller cells display staining across majority of the retina thickness from the ONL to the RGC layers. AP expression in the OPL and the IPL layers is prominent. Although staining in the region distant from the injection site is weaker, AP expression is widespread in the two synaptic layers. Representative photomicrograph from a HEPES buffer mock-infected eye shows no evidence of AP expression. Yellow arrows mark the injection site; red arrows indicate outer plexiform layer (OPL); red arrowheads indicate inner plexiform layer (IPL); green arrows indicate Müller cells; yellow arrowheads indicate RPE. Abbreviations: alkaline phosphatase (AP), inner nuclear layer (INL), outer nuclear layer (ONL), retinal ganglion cell (RGC), retinal pigment epithelium (RPE).

of AAV vector in 30 s. The injection was considered successful when retinal blebs occupied more than half of the retina. Evaluation was performed only in mice that were successfully injected. Following subretinal injection, 1% atropine eyedrops and antibiotic ophthalmic ointment were administered daily for three days. Seven days after injection, the mice were anesthetized with ketamine and xylazine as described previously, and their eyes were examined under microscope. Eyes that exhibited any sign of surgical complications, including anterior or posterior synechia, cataract, vitreous and retinal hemorrhage, and unresolved

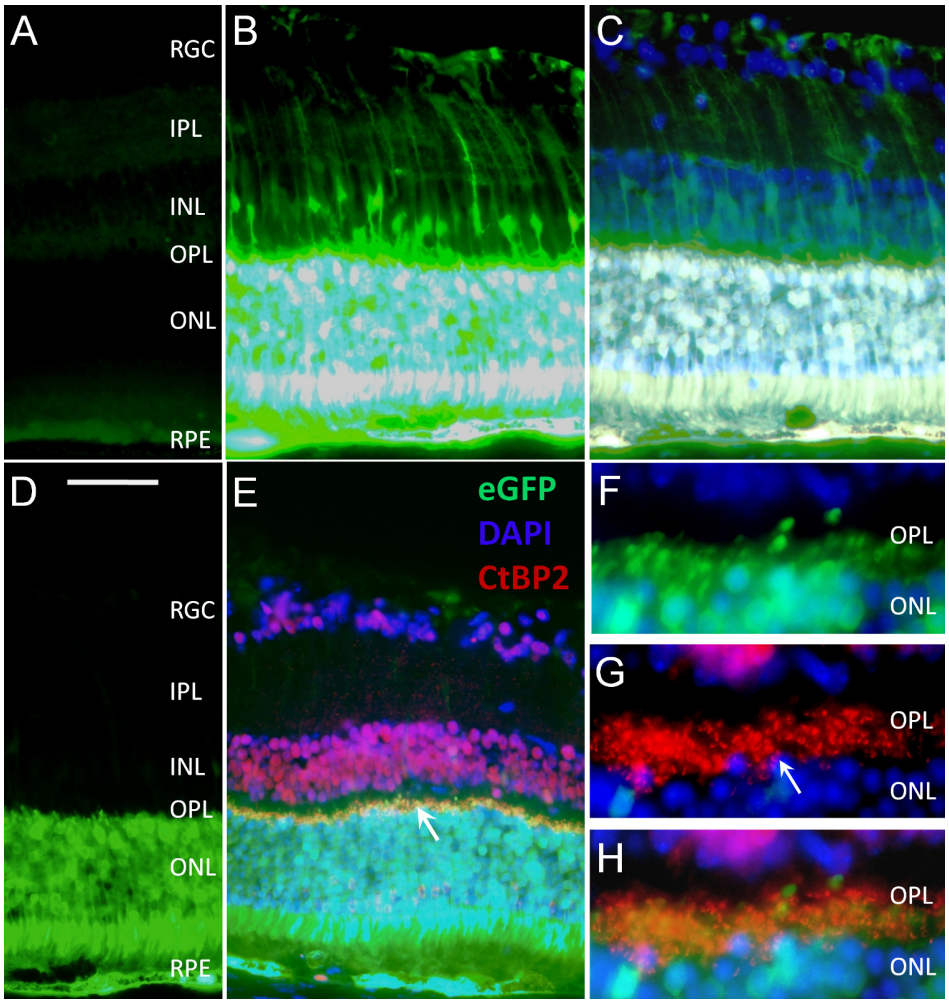


Figure 2. Retinal eGFP expression after subretinal delivery of an AAV-9.CMV.eGFP vector in a 3-month-old *C57BL/6J* mouse. AAV-9 led to widespread (from the injection site, which is close to the posterior pole, to the peripheral retina) and throughout (from the outer retina RPE layer to the inner retina RGC layer) eGFP expression in the mouse retina. The eGFP expression pattern near the injection site and in areas remote from the injection site was similar. The pictures were taken at approximately 300 to 500 µm away from the injection site. **A-C** were taken under the same exposure conditions. **D-H** were taken with a shorter exposure time. **A** is a section from a control eye. **B** shows eGFP expression in the retina, and **C** is a merged picture of **B** and DAPI staining. **B** and **C** show GFP expression in the RPE, photoreceptors (including the outer and inner segment), ONL, OPL, Müller cells in the INL, IPL and RGC layer. Because of a shorter exposure time (**D**), eGFP expression was only seen in the outer retina including RPE and the photoreceptor layer. No expression was observed in the inner retina. **E** is a merged picture of eGFP expression and CtBP2, DAPI staining. In the distal portion of the OPL, colocalization of eGFP expression and CtBP2 staining is evident (arrow). **F, G**, and **H** are enlarged pictures of the OPL. **F**. eGFP expression is evident in the distal portion of the OPL, which is beyond the photoreceptor nuclei (in blue). **G** shows CtBP2 staining (arrow) in the photoreceptor terminals. Panel **H** is a merged picture of eGFP expression and CtBP2, DAPI staining. eGFP expression overlaps with CtBP2 in the photoreceptor terminals in the distal portion of the OPL The calibration bar is 50 µm for **A-E**, and 20 µm for **F-H**. Abbreviations: inner nuclear layer (INL), inner plexiform layer (IPL), outer nuclear layer (ONL), outer plexiform layer (OPL), retinal ganglion cell (RGC), retinal pigment epithelium (RPE).

retinal detachment, were excluded from the study. Such signs were observed in 20% to 30% of the eyes.

*Retinal morphology and gene expression:* For AP and dystrophin expression, mouse eyes were enucleated and snap frozen in liquid nitrogen–cooled isopentane in optimal cutting temperature (OCT) compound (Sakura Finetek Inc., Torrance, CA). Next, 10 µm cryosections were cut along the optic nerve head and stained with hematoxylin and eosin

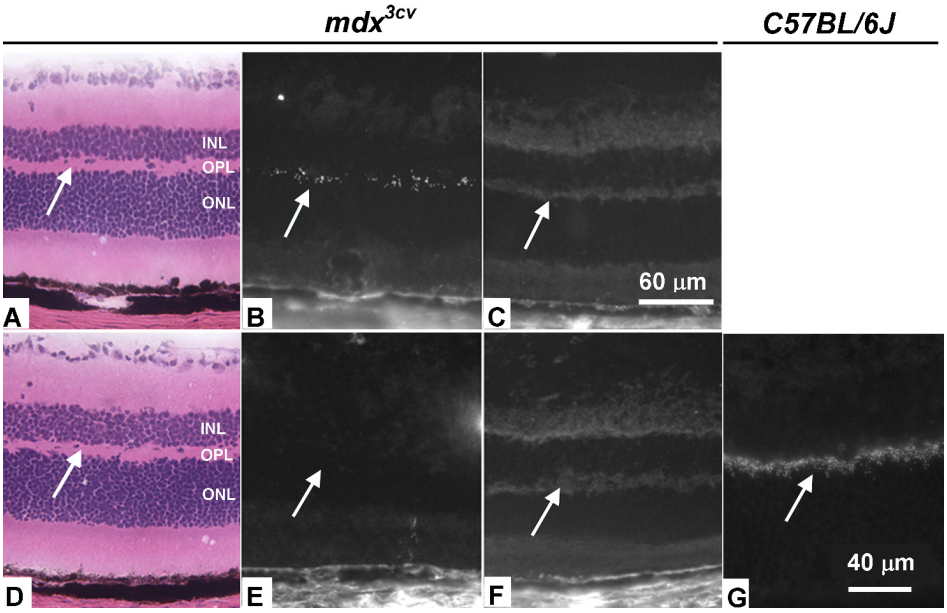


Figure 3. Retinal microdystrophin expression in gene transferred 3-month-old *mdx*$^{3cv}$ mouse. Subretinal delivery of an AAV-9 human microdystrophin vector resulted in efficient OPL transduction in *mdx*$^{3cv}$ mouse retina. **A-F** are from *mdx*$^{3cv}$ mouse eyes, and **G** is from a *C57BL/6J* mouse eye. **A-C** are representative serial sections from an eye infected with AAV-9 microdystrophin vector. **D-F** are representative serial sections from an eye mock-infected with HEPES buffer. **A, D** show retinal structure of *mdx*$^{3cv}$ mouse (H&E staining). **B, E** show immunostaining with the Dys-3 antibody, which recognizes microdystrophin. At 5 weeks after subretinal injection, microdystrophin expression was evident in the injected retina (**B**), but not in the mock-infected eye (**E**). **C** and **F** display immunostaining with the Dys-2 antibody, which recognizes endogenous dystrophin. Neither the AAV-9-infected nor the mock-infected eye showed endogenous dystrophin expression. **G** shows immunostaining with the Dys-2 antibody on the *C57BL/6J* retina. Dystrophin expression is seen in the outer plexiform layer (OPL). Arrows point to the OPL. Abbreviations: inner nuclear layer (INL), outer nuclear layer (ONL).

(H&E) for routine retinal morphology. After endogenous heat labile AP activity was heat inactivated, AAV-9 mediated AP expression was examined by histochemical staining using a previously described protocol [22-24]. Microdystrophin expression was evaluated by immunofluorescence staining according to a previously published protocol [30]. Briefly, cryosections were sequentially blocked with Papain-digested rabbit anti-mouse immunoglobulin and rabbit serum. Then sections were stained with the primary anti-dystrophin antibody and signal was detected with appropriate secondary antibodies. The present study employed 1:30 Dys-2 antibody (Novocastra, Newcastle, UK), which recognizes dystrophin C-terminal domain and 1:20 Dys-3 antibody (Novocastra), which recognizes the hinge 1 region in human dystrophin. Also used was 1:100 Alexa Fluor 594-conjugated goat anti-mouse IgG ($H^+L$) $F(ab')_2$ fragment antibody as the secondary antibody in immunofluorescence staining (Invitrogen, Carlsbad, CA). For eGFP and CtBP2 detection, the eyeballs were first fixed in 4% paraformaldehyde and phosphate-buffer saline (PBS,, 0.01 M phosphate buffer, 0.0027 M potassium chloride and 0.137 M sodium chloride, pH 7.4) then cryoprotected in 30% sucrose/PBS overnight. Next, 10 μm cryosections were stained with 1:200 goat anti-CtBP2 (C-terminal binding protein 2, Santa Cruz, Biotechnology, Santa Cruz, CA) followed by 1:500 Texas Red conjugated donkey anti-goat IgG secondary antibody (Jackson ImmunoResearch, West Grove, PA). Nuclei were revealed with 1:500 4',6-diamidino-2-phenylindole, dihydrocholoride (DAPI, Molecular Probes, Eugene, OR). The specificity of immunostaining was confirmed by staining cryosections in the absence of the primary antibody. Photomicrographs were taken with a digital camera using a Leica fluorescence microscope (DMR, Deerfield, IL).

*Electroretinography:* Retinal function was evaluated at 5 weeks after subretinal injection. Both dark- and light-adapted ERG were examined according to a previously published protocol [31,32].

*Statistical analysis:* Data are presented as mean±standard deviation (mean±SD). Statistical significance was examined with ANOVA followed by the Tukey post hoc test. A p value of less than 0.05 was considered as significant.

## RESULTS

We first examined subretinal AAV-9 AAV.RSV.AP injection in normal *C57BL/6J* mice. Figure 1 shows the representative retinal cross-sections from young (n=6 eyes, 3 weeks post-injection), adult (n=12 eyes, 5 weeks post-injection) and old (n=5 eyes, 5 weeks post-injection) mice. AAV-9 resulted in widespread (peripheral to central to peripheral) and throughout (RPE to retinal ganglion cells [RGC]) AP expression in all age groups (Figure 1A, data not shown for young and old mice). Nevertheless, the highest expression was observed at the injection site (Figure 1A, arrow). AP expression was observed in the RPE, outer nuclear layer (ONL), inner nuclear layer (INL), OPL, inner plexiform layer (IPL), RGC layer and Müller cells but not the outer and inner segments of the photoreceptor (Figure 1C,E-H). Remarkably, two retinal synaptic layers (OPL and IPL) were highly transduced (Figure 1C,E-H). AP expression was not detected in the mock-infected control eyes (5 eyes each for young and adult mice; Figure 1B,D).

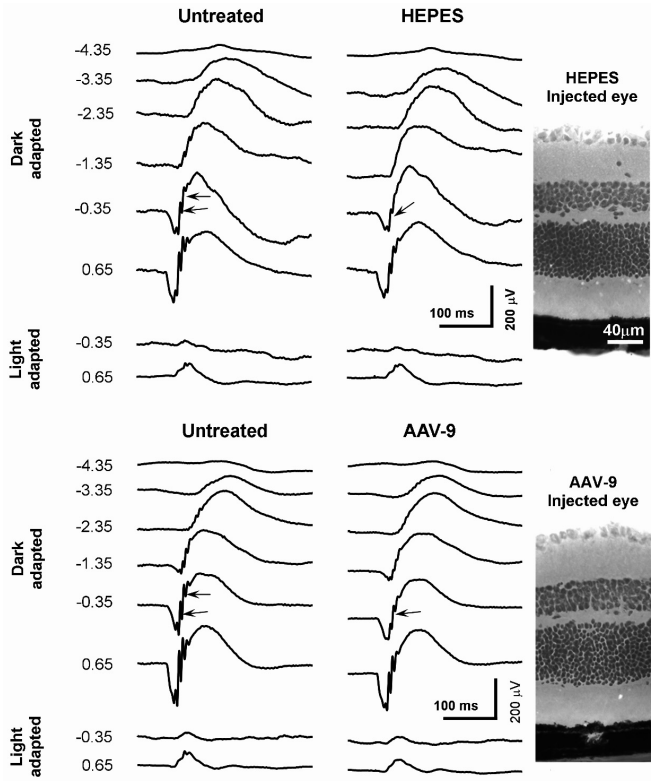


Figure 4. Effects of subretinal delivery of an AAV-9.RSV.AP vector on mouse electroretinogram. Dark-adapted and light-adapted electroretinograms were recorded from 12-month-old *C57BL/6J* mice at 5 weeks after subretinal injection of AAV-9.RSV.AP or HEPES buffer. One eye was injected and the contralateral eye was untreated. Black arrows indicate OPs. The numbers to the left of the ERG signals represent the stimulus light intensity (log cd-s/m$^2$). The background light for light-adaptation was 30 cd/m$^2$.

To exclude the potential bias from the transgene as well as the promoter, we evaluated AAV-9.CMV.eGFP transduction (4 eyes in 2-week-old and 4 eyes in 3-month-old mice). Four weeks after subretinal injection, we observed intense eGFP expression in young and adult groups in the RPE, ONL, INL, OPL, IPL, RGC layers, and Müller cells (Figure 2B,C). Interestingly, we also observed robust expression in the photoreceptors (Figure 2B-E). To further confirm OPL transduction, we stained AAV-9.CMV.eGFP-infected eyes with CtBP2, a marker for the photoreceptor synaptic ribbon (Figure 2 E,G,H). The colocalization of eGFP and CtBP2 strongly suggest that the OPL layer was transduced (Figure 2F,H).

OPL defects are associated with several retinal diseases. To determine whether AAV-9 can be used to deliver a therapeutic gene to the OPL, we performed subretinal injection in *mdx*$^{3cv}$ mice using AAV-9.CMV.ΔR4–23/ΔC vector. *Mdx*$^{3cv}$ mice are models for DMD, a lethal childhood genetic disease caused by mutations in the dystrophin gene [33,34]. Besides muscle disease, DMD patients also suffer from pathology in other systems such the central nerve system. A 260 kDa dystrophin isoform (Dp260) is normally expressed in the OPL. In the eyes of DMD patients and *mdx*$^{3cv}$ mice, Dp260 expression is lost [35-37]. The absence of Dp260 has been associated with the abnormal ERG seen in DMD patients.

The 3.8 kb ΔR4–23/ΔC microgene encodes a highly truncated dystrophin. This microgene has been extensively studied as a candidate gene for DMD gene therapy [28]. At 5 weeks after subretinal injection (n=5 mice; AAV-9.CMV.ΔR4–23/ΔC to one eye and HEPES buffer to the contralateral eye), we evaluated dystrophin expression by immunofluorescence staining. Two epitope-specific antibodies were used in the study. The Dys-2 antibody recognizes endogenous Dp260 in the wild type retina (Figure 3G) [38], while the Dys-3 antibody only reacts with microdystrophin. Consistent with our findings in reporter AAV vector-infected normal eyes, we observed efficient OPL transduction in the eyes of AAV-9.CMV.ΔR4–23/ΔC infected *mdx*$^{3cv}$ mice (Figure 3B,C). No dystrophin was detected in HEPES buffer-injected eyes (Figure 3E,F).

Next, we studied whether subretinal AAV-9 injection causes acute retinal damage. At 5 weeks after subretinal injection (AAV-9.RSV.AP or HEPES) in adult and old C57BL/6J mice (n=5 for each age group), we examined retinal histology and recorded dark-adapted and light-adapted ERGs. Compared with untreated eyes, neither HEPES buffer injection nor AAV-9.RSV.AP injection resulted in appreciable morphology alterations (Figure 4). In each age group, the thresholds and amplitudes of the dark-adapted ERG a-wave, dark-adapted b-wave and light-adapted b-wave of the AAV-9 or HEPES injected eyes were comparable to those of the untreated eyes ($p>0.05$, Figure 4, Figure 5, and Figure 6).

On the ascending limb of dark-adapted b-wave, the amplitude of the oscillatory potentials (OPs) in the AAV-9 vector injected eyes appeared smaller than the untreated eyes (Figure 4). However, similar reduction was also observed in HEPES-injected eyes.

## DISCUSSION

AAV-mediated gene therapy holds great promise for rescuing vision loss in retinal degenerative diseases. Remarkable progress has been made in animal models and human patients [1,2,4,6-8]. However, most studies have focused on diseases that primarily affect the photoreceptor, RPE, and RGC layer.

There are two synaptic layers in the retina including the OPL in the outer retina and the IPL in the inner retina. The OPL and IPL are indispensable for mediating visual signal transmission. While no human diseases have been associated with the IPL, several retinal diseases originate in as well as primarily affect the OPL. Examples of these diseases include congenital stationary night blindness, retinoschisis, DMD retinopathy, and melanoma-associated retinopathy [14-18]. Gene therapy for these diseases is largely dependent on a vector that can efficiently deliver the therapeutic genes to the OPL.

Several different AAV serotypes have been evaluated for retinal gene delivery. In this study we examined AAV-9 transduction in young, adult, and old mice. Consistent with recent publications from other investigators, we observed robust AAV-9 transduction in the outer retina (RPE and ONL), inner retina (Müller cells), and RGC layers [12,13]. Surprisingly, we also observed quite efficient and widespread transduction in the synaptic layers (Figure 1, Figure 2, and Figure 3). A colocalization study suggested that transduction occurred in the photoreceptor terminals, but not in the bipolar cell and horizontal cell dendrites in the OPL (Figure 2).

To explore therapeutic gene delivery to the OPL we delivered AAV-9.CMV.ΔR4–23/ΔC to adult *mdx*$^{3cv}$ mice. We focused on transgene expression rather than functional correction in this study. Consistent with our findings in normal mice, we observed robust microdystrophin expression in the OPL. Taken together, our results suggest that AAV-9-mediated OPL transduction represents a promising approach to treat retinal diseases that are related to OPL defects.

It is important to understand whether subretinal administration of a new viral vector causes any side effects. We found that subretinal delivery of AAV-9 did not alter retinal structure. In addition, rod and cone photoreceptor and bipolar cell functions were not affected by subretinal AAV-9 injection (Figure 4, Figure 5, and Figure 6). Interestingly the OPs, highly sensitive functional indicators of the inner retina [39], were reduced following AAV-9 injection. Since similar reductions were also observed in HEPES-buffer-injected eyes. We suspect that the OP reduction may relate to the injection procedure rather than AAV-9 vector.

Taken together, our data suggest that AAV-9 is a potent vector for retina gene delivery, and subretinal administration does not cause acute damage. Efficient transduction of the photoreceptor terminals opens the door to develop AAV-9

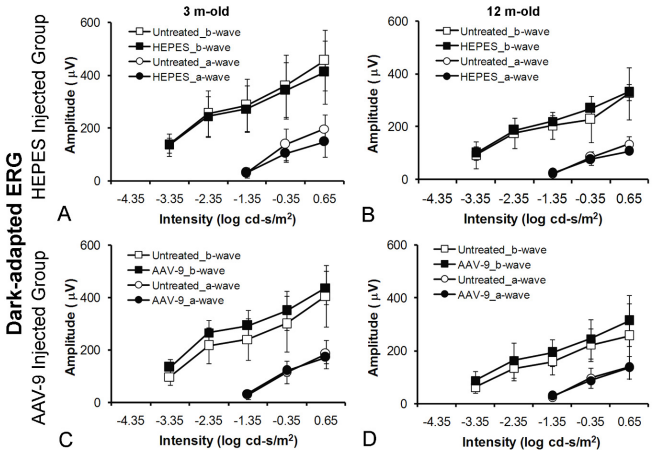


Figure 5. Dark-adapted ERG a-wave and b-wave responses-intensity curves in *C57BL/6J* mice. In all animals, one eye was injected subretinally while the contralateral eye was untreated. **A, B** show HEPES-treated mice and **C, D** show AAV-9.RSV.AP-injected mice. The left column shows the 3-month-old groups (n=5 for each group) and the right column shows the 12-month-old groups (n=5 for each group). The filled symbols represent the injected eyes, and the open symbols represent the untreated eyes. Error bars indicate the standard deviation from the mean (mean±SD).

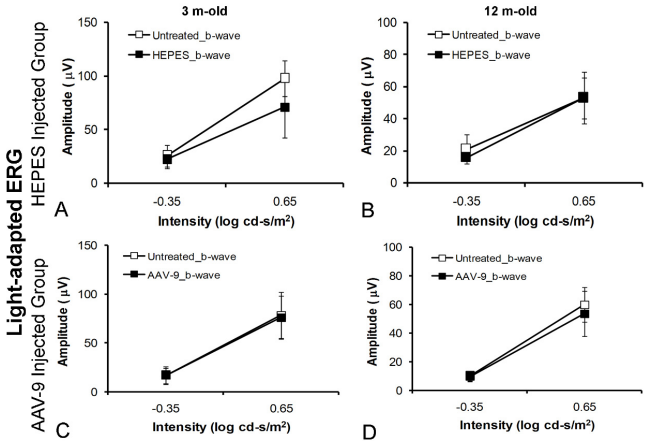


Figure 6. Light-adapted ERG b-wave responses-intensity curves in *C57BL/6J* mice. In all the animals, one eye was injected subretinally while the contralateral eye was not treated. **A, B** show HEPES-treated mice and **C, D** show AAV-9.RSV.AP-injected mice. The left column shows the 3-month-old groups (n=5 for each group), and the right column shows the 12-month-old groups (n=5 for each group). The filled symbols represent the injected eyes, and the open symbols represent the untreated eyes. Background light was 30 cd/m$^2$. Error bars indicate the standard deviation from the mean (mean±SD).

gene therapy for degenerative retinal diseases that affect this synaptic structure.

## ACKNOWLEDGMENTS

This work was supported in part by University of Missouri Research Board, an unrestricted grant from Research to Prevent Blindness, Inc. (New York, NY) to the Department of Ophthalmology, University of Missouri-Columbia, National Institutes of Health AR-49419 (D.D.), and Muscular Dystrophy Association (D.D.). We thank Dr. Jijing Pang for sharing subretinal injection technique, Dr. Lixing W. Reneker for help with histology studies, and Mrs. Chun Long for technical assistance. We also thank Dr. James M. Wilson for providing the AAV-9 packaging plasmid pRep2/Cap9.

## REFERENCES

1. Ali RR, Sarra GM, Stephens C, Alwis MD, Bainbridge JW, Munro PM, Fauser S, Reichel MB, Kinnon C, Hunt DM, Bhattacharya SS, Thrasher AJ. Restoration of photoreceptor ultrastructure and function in retinal degeneration slow mice by gene therapy. Nat Genet 2000; 25:306-10. [PMID: 10888879]
2. Acland GM, Aguirre GD, Ray J, Zhang Q, Aleman TS, Cideciyan AV, Pearce-Kelling SE, Anand V, Zeng Y, Maguire AM, Jacobson SG, Hauswirth WW, Bennett J. Gene therapy restores vision in a canine model of childhood blindness. Nat Genet 2001; 28:92-5. [PMID: 11326284]
3. Allocca M, Tessitore A, Cotugno G, Auricchio A. AAV-mediated gene transfer for retinal diseases. Expert Opin Biol Ther 2006; 6:1279-94. [PMID: 17223737]
4. Alexander JJ, Umino Y, Everhart D, Chang B, Min SH, Li Q, Timmers AM, Hawes NL, Pang JJ, Barlow RB, Hauswirth WW. Restoration of cone vision in a mouse model of achromatopsia. Nat Med 2007; 13:685-7. [PMID: 17515894]
5. Maguire AM, Simonelli F, Pierce EA, Pugh EN Jr, Mingozzi F, Bennicelli J, Banfi S, Marshall KA, Testa F, Surace EM, Rossi S, Lyubarsky A, Arruda VR, Konkle B, Stone E, Sun J, Jacobs J, Dell'Osso L, Hertle R, Ma JX, Redmond TM, Zhu X, Hauck B, Zelenaia O, Shindler KS, Maguire MG, Wright JF, Volpe NJ, McDonnell JW, Auricchio A, High KA, Bennett J. Safety and efficacy of gene transfer for Leber's congenital amaurosis. N Engl J Med 2008; 358:2240-8. [PMID: 18441370]
6. Bainbridge JW, Smith AJ, Barker SS, Robbie S, Henderson R, Balaggan K, Viswanathan A, Holder GE, Stockman A, Tyler N, Petersen-Jones S, Bhattacharya SS, Thrasher AJ, Fitzke FW, Carter BJ, Rubin GS, Moore AT, Ali RR. Effect of gene therapy on visual function in Leber's congenital amaurosis. N Engl J Med 2008; 358:2231-9. [PMID: 18441371]
7. Cideciyan AV, Aleman TS, Boye SL, Schwartz SB, Kaushal S, Roman AJ, Pang JJ, Sumaroka A, Windsor EA, Wilson JM, Flotte TR, Fishman GA, Heon E, Stone EM, Byrne BJ, Jacobson SG, Hauswirth WW. Human gene therapy for RPE65 isomerase deficiency activates the retinoid cycle of vision but with slow rod kinetics. Proc Natl Acad Sci USA 2008; 105:15112-7. [PMID: 18809924]
8. Hauswirth WW, Aleman TS, Kaushal S, Cideciyan AV, Schwartz SB, Wang L, Conlon T, Boye SL, Flotte TR, Byrne B, Jacobson SG. Treatment of leber congenital amaurosis due to RPE65 mutations by ocular subretinal injection of adeno-associated virus gene vector: short-term results of a phase I trial. Hum Gene Ther 2008; 19:979-90. [PMID: 18774912]
9. Gao G, Vandenberghe LH, Wilson JM. New recombinant serotypes of AAV vectors. Curr Gene Ther 2005; 5:285-97. [PMID: 15975006]
10. Rabinowitz JE, Rolling F, Li C, Conrath H, Xiao W, Xiao X, Samulski RJ. Cross-packaging of a single adeno-associated virus (AAV) type 2 vector genome into multiple AAV serotypes enables transduction with broad specificity. J Virol 2002; 76:791-801. [PMID: 11752169]
11. Yang GS, Schmidt M, Yan Z, Lindbloom JD, Harding TC, Donahue BA, Engelhardt JF, Kotin R, Davidson BL. Virus-mediated transduction of murine retina with adeno-associated virus: effects of viral capsid and genome size. J Virol 2002; 76:7651-60. [PMID: 12097579]
12. Allocca M, Mussolino C, Garcia-Hoyos M, Sanges D, Iodice C, Petrillo M, Vandenberghe LH, Wilson JM, Marigo V, Surace EM, Auricchio A. Novel adeno-associated virus serotypes efficiently transduce murine photoreceptors. J Virol 2007; 81:11372-80. [PMID: 17699581]
13. Lebherz C, Maguire A, Tang W, Bennett J, Wilson JM. Novel AAV serotypes for improved ocular gene transfer. J Gene Med 2008; 10:375-82. [PMID: 18278824]
14. Dryja TP, McGee TL, Berson EL, Fishman GA, Sandberg MA, Alexander KR, Derlacki DJ, Rajagopalan AS. Night blindness and abnormal cone electroretinogram ON responses in patients with mutations in the GRM6 gene encoding mGluR6. Proc Natl Acad Sci USA 2005; 102:4884-9. [PMID: 15781871]
15. Miyake Y, Yagasaki K, Horiguchi M, Kawase Y, Kanda T. Congenital stationary night blindness with negative electroretinogram. A new classification. Arch Ophthalmol 1986; 104:1013-20. [PMID: 3488053]
16. Fitzgerald KM, Cibis GW, Giambrone SA, Harris DJ. Retinal signal transmission in Duchenne muscular dystrophy: evidence for dysfunction in the photoreceptor/depolarizing bipolar cell pathway. J Clin Invest 1994; 93:2425-30. [PMID: 8200977]
17. Alexander KR, Fishman GA, Peachey NS, Marchese AL, Tso MO. 'On' response defect in paraneoplastic night blindness with cutaneous malignant melanoma. Invest Ophthalmol Vis Sci 1992; 33:477-83. [PMID: 1544774]
18. Chang B, Heckenlively JR, Bayley PR, Brecha NC, Davisson MT, Hawes NL, Hirano AA, Hurd RE, Ikeda A, Johnson BA, McCall MA, Morgans CW, Nusinowitz S, Peachey NS, Rice DS, Vessey KA, Gregg RG. The nob2 mouse, a null mutation in Cacna1f: anatomical and functional abnormalities in the outer retina and their consequences on ganglion cell visual responses. Vis Neurosci 2006; 23:11-24. [PMID: 16597347]
19. Zhang SH, Wu JH, Wu XB, Dong XY, Liu XJ, Li CY, Qian H. Distinctive gene transduction efficiencies of commonly used viral vectors in the retina. Curr Eye Res 2008; 33:81-90. [PMID: 18214745]
20. Gao G, Vandenberghe LH, Alvira MR, Lu Y, Calcedo R, Zhou X, Wilson JM. Clades of Adeno-associated viruses are widely disseminated in human tissues. J Virol 2004; 78:6381-8. [PMID: 15163731]
21. Foust KD, Nurre E, Montgomery CL, Hernandez A, Chan CM, Kaspar BK. Intravascular AAV9 preferentially targets

neonatal neurons and adult astrocytes. Nat Biotechnol 2009; 27:59-65. [PMID: 19098898]

22. Bostick B, Ghosh A, Yue Y, Long C, Duan D. Systemic AAV-9 transduction in mice is influenced by animal age but not by the route of administration. Gene Ther 2007; 14:1605-9. [PMID: 17898796]
23. Ghosh A, Yue Y, Long C, Bostick B, Duan D. Efficient whole-body transduction with trans-splicing adeno-associated viral vectors. Mol Ther 2007; 15:750-5. [PMID: 17264855]
24. Duan D, Yue Y, Yan Z, Yang J, Engelhardt JF. Endosomal processing limits gene transfer to polarized airway epithelia by adeno-associated virus. J Clin Invest 2000; 105:1573-87. [PMID: 10841516]
25. Liu M, Yue Y, Harper SQ, Grange RW, Chamberlain JS, Duan D. Adeno-associated virus-mediated microdystrophin expression protects young mdx muscle from contraction-induced injury. Mol Ther 2005; 11:245-56. [PMID: 15668136]
26. Pacak CA, Mah CS, Thattaliyath BD, Conlon TJ, Lewis MA, Cloutier DE, Zolotukhin I, Tarantal AF, Byrne BJ. Recombinant adeno-associated virus serotype 9 leads to preferential cardiac transduction in vivo. Circ Res 2006; 99:e3-9. [PMID: 16873720]
27. Inagaki K, Fuess S, Storm TA, Gibson GA, McTiernan CF, Kay MA, Nakai H. Robust systemic transduction with AAV9 vectors in mice: efficient global cardiac gene transfer superior to that of AAV8. Mol Ther 2006; 14:45-53. [PMID: 16713360]
28. Harper SQ, Hauser MA, DelloRusso C, Duan D, Crawford RW, Phelps SF, Harper HA, Robinson AS, Engelhardt JF, Brooks SV, Chamberlain JS. Modular flexibility of dystrophin: implications for gene therapy of Duchenne muscular dystrophy. Nat Med 2002; 8:253-61. [PMID: 11875496]
29. Pang JJ, Chang B, Kumar A, Nusinowitz S, Noorwez SM, Li J, Rani A, Foster TC, Chiodo VA, Doyle T, Li H, Malhotra R, Teusner JT, McDowell JH, Min SH, Li Q, Kaushal S, Hauswirth WW. Gene therapy restores vision-dependent behavior as well as retinal structure and function in a mouse model of RPE65 Leber congenital amaurosis. Mol Ther 2006; 13:565-72. [PMID: 16223604]
30. Yue Y, Li Z, Harper SQ, Davisson RL, Chamberlain JS, Duan D. Microdystrophin gene therapy of cardiomyopathy restores dystrophin-glycoprotein complex and improves sarcolemma integrity in the mdx mouse heart. Circulation 2003; 108:1626-32. [PMID: 12952841]
31. Lei B, Tullis GE, Kirk MD, Zhang K, Katz ML. Ocular phenotype in a mouse gene knockout model for infantile neuronal ceroid lipofuscinosis. J Neurosci Res 2006; 84:1139-49. [PMID: 16881055]
32. Lei B, Yao G, Zhang K, Hofeldt KJ, Chang B. Study of rod- and cone-driven oscillatory potentials in mice. Invest Ophthalmol Vis Sci 2006; 47:2732-8. [PMID: 16723493]
33. Pillers DA, Weleber RG, Woodward WR, Green DG, Chapman VM, Ray PN. mdxCv3 mouse is a model for electroretinography of Duchenne/Becker muscular dystrophy. Invest Ophthalmol Vis Sci 1995; 36:462-6. [PMID: 7843915]
34. Pillers DA, Weleber RG, Green DG, Rash SM, Dally GY, Howard PL, Powers MR, Hood DC, Chapman VM, Ray PN, Woodward WR. Effects of dystrophin isoforms on signal transduction through neural retina: genotype-phenotype analysis of duchenne muscular dystrophy mouse mutants. Mol Genet Metab 1999; 66:100-10. [PMID: 10068512]
35. Schmitz F, Drenckhahn D. Localization of dystrophin and beta-dystroglycan in bovine retinal photoreceptor processes extending into the postsynaptic dendritic complex. Histochem Cell Biol 1997; 108:249-55. [PMID: 9342619]
36. Jastrow H, Koulen P, Altrock WD, Kroger S. Identification of a beta-dystroglycan immunoreactive subcompartment in photoreceptor terminals. Invest Ophthalmol Vis Sci 2006; 47:17-24. [PMID: 16384939]
37. Pillers DA, Bulman DE, Weleber RG, Sigesmund DA, Musarella MA, Powell BR, Murphey WH, Westall C, Panton C, Becker LE, Worton RG, Ray PN. Dystrophin expression in the human retina is required for normal function as defined by electroretinography. Nat Genet 1993; 4:82-6. [PMID: 8513332]
38. Dalloz C, Claudepierre T, Rodius F, Mornet D, Sahel J, Rendon A. Differential distribution of the members of the dystrophin glycoprotein complex in mouse retina: effect of the mdx(3Cv) mutation. Mol Cell Neurosci 2001; 17:908-20. [PMID: 11358487]
39. Wachtmeister L. Oscillatory potentials in the retina: what do they reveal. Prog Retin Eye Res 1998; 17:485-521. [PMID: 9777648]

The print version of this article was created on 15 July 2009. This reflects all typographical corrections and errata to the article through that date. Details of any changes may be found in the online version of the article.